# Stage-specific vascular markers revealed by phage display in a mouse model of pancreatic islet tumorigenesis

Johanna A. Joyce,[1,3] Pirjo Laakkonen,[2,3,4] Michele Bernasconi,[2,5] Gabriele Bergers,[1,6] Erkki Ruoslahti,[2,*] and Douglas Hanahan[1,*]

[1]Department of Biochemistry and Biophysics, Diabetes and Comprehensive Cancer Centers, University of California, San Francisco, 513 Parnassus Avenue, San Francisco, California 94143
[2]Cancer Research Center, The Burnham Institute, 10901 North Torrey Pines Road, La Jolla, California 92037
[3]These authors contributed equally to this work.
[4]Present address: Molecular/Cancer Biology Laboratory, Biomedicum Helsinki, University of Helsinki, P.O.B. 63 (Haartmaninkatu 8), FIN-00014 Helsinki, Finland.
[5]Present address: Functional Genomics Unit, Divisions of Infectious Diseases and Oncology, The University Children's Hospital of Zürich, August-Forel Strasse 1 CH-8008 Zürich, Switzerland.
[6]Present address: Department of Neurological Surgery, University of California, San Francisco, 513 Parnassus Avenue, San Francisco, California 94143.
*Correspondence: dh@biochem.ucsf.edu (D.H.); ruoslahti@burnham.org (E.R.)

## Summary

**The vasculature in the angiogenic stages of a mouse model of pancreatic islet carcinogenesis was profiled in vivo with phage libraries that display short peptides. We characterized seven peptides distinguished by their differential homing to angiogenic progenitors, solid tumors, or both. None homed appreciably to normal pancreatic islets or other organs. Five peptides selectively homed to neoplastic lesions in the pancreas and not to islet β cell tumors growing subcutaneously, xenotransplant tumors from a human cancer cell line, or an endogenously arising squamous cell tumor of the skin. Three peptides with distinctive homing to angiogenic islets, tumors, or both colocalized with markers that identify endothelial cells or pericytes. One peptide is homologous with pro-PDGF-B, which is expressed in endothelial cells, while its receptor is expressed in pericytes.**

## Introduction

Angiogenesis, the formation of new blood vessels, is essential for tumor growth. The transition from normal to neoplastic vasculature during tumorigenesis has been termed the "angiogenic switch," and both positive and negative regulators of the switch have been identified (Hanahan and Folkman, 1996). The vascular anatomy of tumors is typically distinct from that of normal tissues (Carmeliet and Jain, 2000). In contrast to their normal counterparts, tumor vessels are tortuous and dilated and show reduced vessel integrity. Tumor vessels often have numerous fenestrae or discontinuities, loose interendothelial junctions, and a discontinuous or absent basement membrane, collectively resulting in vessel leakiness (Carmeliet and Jain, 2000; Hashizume et al., 2000).

We are only beginning to understand the molecular events underlying the pronounced abnormalities evident in the angiogenic vasculature of tumors and progenitor lesions. Previous studies have shown that a number of genes are upregulated during the transition from normal to tumor blood vessels, including the integrins αvβ3, αvβ5, and α5β1; several matrix metalloproteinases; and various endothelial growth factor receptors (Hanahan and Folkman, 1996; Ruoslahti, 2002). Recently, St. Croix et al. further showed, using a comparative RNA expression profiling technology (SAGE), that a number of genes or EST's were selectively expressed or upregulated in the tumor endothelium of human colorectal cancer, relative to the corresponding normal colonic vasculature (St. Croix et al., 2000). This approach relied on substantive differences in gene expression to identify tumor-specific endothelial markers, which will likely only reveal a subset of alterations that distinguish normal and tumor blood vessels. Specific binding of phage from libraries that can display more than a billion random peptide sequences offers a complementary approach for comparative screening. In vivo phage display screening has proven to be a powerful method for un-

### SIGNIFICANCE

**While there is abundant evidence that tumor vasculature is functionally and morphologically aberrant, we show herein using a peptide epitope profiling technology that the angiogenic vasculature in premalignant lesions is distinguishable from normal as well as tumor vessels in a model of multistage tumorigenesis. Moreover, both angiogenic progenitor and tumor vessels in the pancreas have molecular signatures distinct from tumors growing in or under the skin, even of the analogous cell type. The stage and organ specificities of particular homing peptides may prove instructive about mechanisms regulating the neovasculature in different pathways of tumorigenesis, suggest means to detect and distinguish premalignant and malignant lesions noninvasively, and predict differential sensitivity to therapeutic agents targeting angiogenesis.**

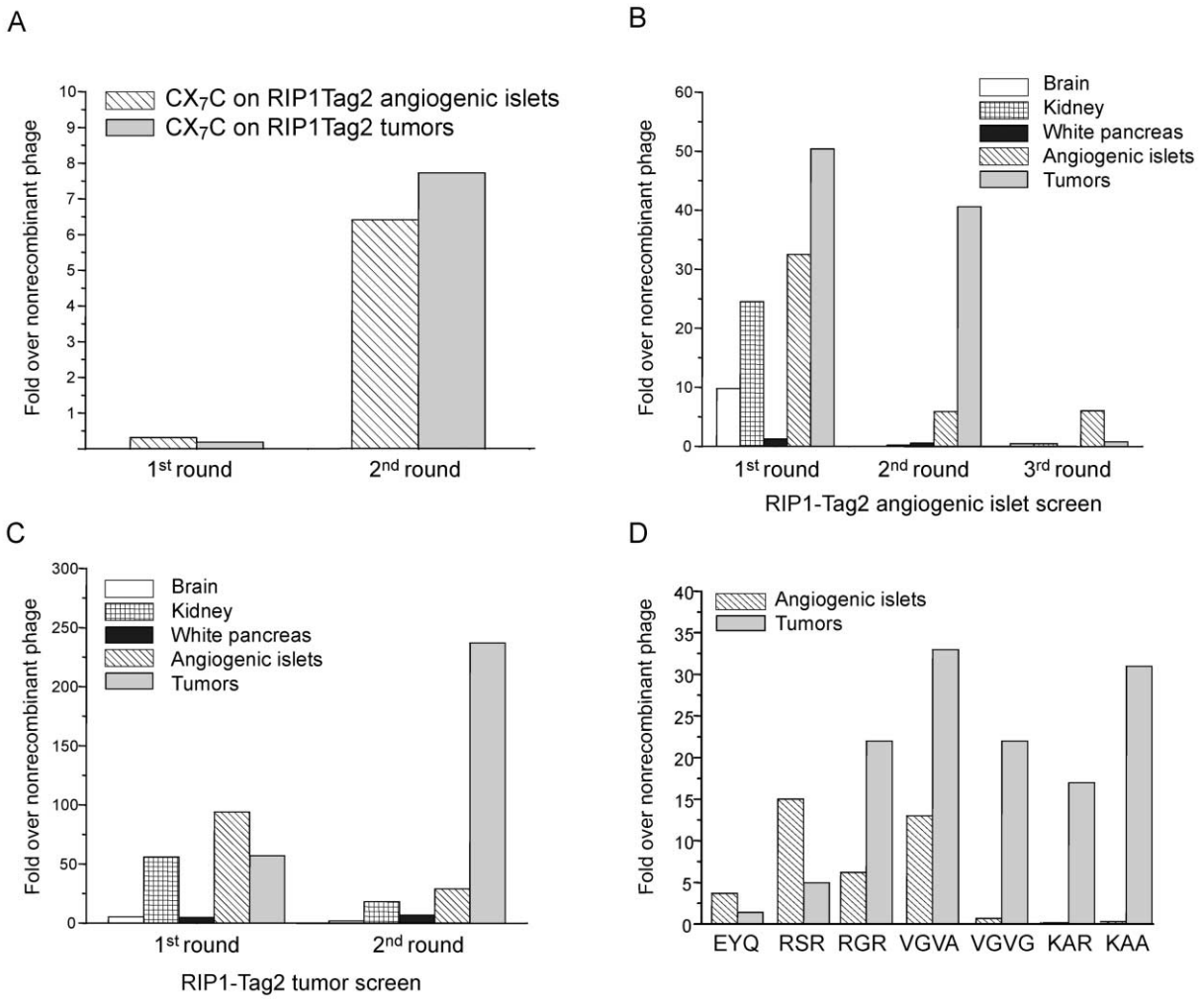


**Figure 1.** Isolation of stage-specific phage using ex vivo and in vivo phage display

**A:** Ex vivo screening on cells derived from RIP1-Tag2 angiogenic islets or tumors using the $CX_7C$ peptide library displayed on T7 phage. The enriched phage pools were used for subsequent in vivo homing to RIP1-Tag2 angiogenic islets (three rounds of selection) (**B**) and tumors (two rounds of selection) (**C**). **D:** In vivo homing of individual phage to RIP1-Tag2 angiogenic islets and tumors.

covering differences among individual vascular beds in normal organs (Pasqualini and Ruoslahti, 1996; Rajotte et al., 1998) and has also yielded peptides that specifically home to blood vessels or lymphatics in tumors (Arap et al., 1998; Laakkonen et al., 2002; Porkka et al., 2002). The targets for these peptides in blood vessels include the $\alpha v\beta 3$ and $\alpha v\beta 5$ integrins (Arap et al., 1998) and aminopeptidase N (Pasqualini et al., 2000).

In this and a companion study (Hoffman et al., 2003 [this issue of *Cancer Cell*]), we set out to use phage-display profiling to ask whether additional levels of neoplastic vascular specialization might exist in tumor development. We sought to distinguish the vessels of premalignant angiogenic lesions from those of angiogenic solid tumors and to examine whether differences exist between angiogenic vessels of tumors developing in different organs. Previous studies have profiled differences between normal blood vessels and the vasculature of transplanted tumors in immunodeficient mice. Unlike these transplanted tumors, transgenic tumor models provide an opportunity to examine pre-neoplastic changes unfolding in different organs in a more physiologically relevant microenvironment.

We used a prototypical mouse model of multistage tumorigenesis, the RIP1-Tag2 transgenic model of islet cell carcinoma (Hanahan, 1985), to address our hypothesis that the vasculature of pre-neoplastic lesions differs from that of established tumors. RIP1-Tag2 transgenic mice express the SV40 T antigens (Tag) under the control of the insulin gene promoter, which elicits the sequential development of tumors in the islets of Langerhans over a period of 12–14 weeks. Hyperplastic islets begin to appear at around 4 weeks of age, and angiogenesis is activated a few weeks later in a subset of the hyperplastic islets, producing angiogenic (dysplastic) islets (Bergers et al., 1998; Folkman et al., 1989). Solid tumors form beginning at 9 to 10 weeks, initially presenting as small nodules that grow and progress to large islet tumors with well-defined margins, as well as two classes of invasive carcinoma (Lopez and Hanahan, 2002). We set out to identify stage-specific molecular markers accessible via the circulation, either on the surface of endothelial cells, their perivascular support cells (pericytes and smooth muscle cells), or even tumor cells themselves (as a result of the hemorrhagic,

leaky angiogenic vasculature). We successfully selected phage pools that homed preferentially to different stages during RIP1-Tag2 tumorigenesis. In addition to "pan-angiogenic" markers shared by many types of tumors, we identified vascular target molecules that are characteristic of this tumor's tissue of origin and are not expressed in the vessels of several tumor types growing in or under the skin. We have begun to investigate the binding partners for these peptides and present evidence linking one peptide to a vascular signaling circuit involving PDGF ligands expressed in endothelial cells and their receptor PDGFRβ, expressed in pericytes of the angiogenic vasculature.

## Results

### Isolation of stage-specific phage from RIP1-Tag2 mice

RIP1-Tag2 mice develop multifocal angiogenic islet progenitors and then solid tumors in a stepwise manner, such that at 12 weeks of age, each mouse will typically have approximately 50 angiogenic islets and 2–6 small tumors. This circumstance allowed us to use 12-week-old mice to select for phage binding to angiogenic islet progenitors and/or tumors in the same mouse. In order to enrich for phage that bind to RIP1-Tag2 target cells (endothelial, perivascular, and tumor), we included a pre-selection step (Laakkonen et al., 2002; Porkka et al., 2002) on cell suspensions prepared from pancreatic lesions. Two rounds of ex vivo selection from a $CX_7C$ peptide library on cell suspensions from angiogenic islets or solid tumors yielded phage pools that bound 7- to 8-fold over a control, nonrecombinant phage to their respective target cells (Figure 1A). These enriched phage pools were used in subsequent in vivo rounds to select for phage that would home specifically to either angiogenic islets or tumors in RIP1-Tag2 mice.

Three rounds of in vivo selection on angiogenic islets resulted in a phage pool that selectively homed to angiogenic islets. The homing to the islets was 7-fold higher than to tumors in the same mouse (Figure 1B). There was no homing to control organs. The tumor selection yielded a pool that showed an 8-fold preference for tumors versus angiogenic islets in the same mouse following two rounds of in vivo selection (Figure 1C).

Sequencing of phage from the selected pools identified a number of peptide sequences that were represented more than once, and these were tested for their ability to bind cell suspensions prepared from angiogenic islets and tumors. Six of the phage selected for further analysis were from the tumor screen (referred to as KAA, RGR, RSR, VGVA, VGVG, and KAR), and one (EYQ) was picked from the angiogenic screen. Peptide sequences corresponding to each of these peptide motifs are shown in Table 1. All of these peptides are linear, although the phage library used here ($CX_7C$) was designed to express peptides cyclized by a covalent bond between two cysteine residues. However, a library of this design does contain a minority of linear peptides. A stop codon occurring within the random insert will cause truncation of the peptide, and a frameshift mutation frequently changes the second cysteine into valine. It may be that the target molecules in the RIP1-Tag2 tumors selected for linear peptides. In the companion study (Hoffman et al., 2003), the same library yielded cyclic homing peptides. The RIP1-Tag2 homing phage fall into three classes based on their homing either to angiogenic islets or to tumors in vivo (Figure 1D) and their ex vivo binding patterns: tumor-selective phage (KAA, KAR, and VGVG), angiogenic islet-selective phage (RSR and EYQ), and phage that home to both types of angiogenic lesions (VGVA and RGR). Some of the selected peptides that share similar peptide motifs also display similar homing patterns. For example, KAA and KAR (CKAAKNK and CKGAKAR = XBXXBXB, where B represents basic residues and X denotes uncharged residues) both preferentially home to tumors over angiogenic islets. However, other related peptides such as RGR and RSR (CRGRRST and CRSRKG = XBXBBX) have quite different homing capabilities. Interestingly, all of these peptides are distinct from those found previously in phage display screens of transplant tumors (Arap et al., 1998; Laakkonen et al., 2002; Porkka et al., 2002).

### Stage-specific homing of fluorescein-conjugated peptides

To confirm that the selective phage homing was due to the displayed peptide sequences, we studied the localization of fluorescein-conjugated peptides after intravenous injection; one peptide from each homing class was selected for detailed analysis. We used 8-week-old RIP1-Tag2 mice to examine peptide localization during the angiogenic switch and 12-week-old RIP1-Tag2 mice to visualize both angiogenic islets and tumors.

The observed peptide localization profiles in each case closely mimicked that of the cognate phage, as shown in Figure 1D, with each peptide falling into the same of the three homing classes. Figure 2 illustrates the peptide localization for these three representative fluorescein-conjugated peptides: RSR (angiogenic-selective), KAA (tumor-selective), and RGR (angiogenic- and tumor-homing). RSR shows abundant accumulation in RIP1-Tag2 angiogenic islets (Figure 2B) but little or no localization in tumors (Figure 2C) or normal islets (Figure 2A). KAA shows abundant localization in RIP1-Tag2 tumors (Figure 2F) but little or no localization in angiogenic islets (Figure 2E) or normal islets (Figure 2D). Finally, RGR localizes in both RIP1-Tag2 angiogenic islets (Figure 2H) and tumors (Figure 2I) but there is little or no peptide in normal islets (Figure 2G). It was somewhat unexpected that RSR, which was selected from the tumor phage screening, preferentially bound to angiogenic islets. It seems that the epitope this peptide binds to is present both in tumors and angiogenic islets, but is more abundant in angiogenic islets. This result could also be indicative of the heterogeneity of the pools of angiogenic islets or tumors isolated by gross examination, in which there are multiple lesions of differing grades within each group. Hence, a gross selection of the tumor pool may in fact include some large, advanced angiogenic islets that can only be definitively distinguished by histological grading, which was performed in conjunction with the peptide homing to the different lesions.

Homing of the peptides to the pancreatic islet lesions was specific: little or no homing was detected in normal islets, brain, liver, lung, and spleen (Figures 2K and 2L and data not shown). Fluorescence was detected in kidney, presumably as a result of uptake from glomerular filtrate (Figure 2J). Representative figures of control tissues from a RIP1-Tag2 mouse injected with fluorescein-conjugated RGR peptide are shown in Figures 2J–2L. A similar absence of fluorescence in control tissues was observed for all other injected peptides (data not shown). In addition, control peptides did not show specific homing to any of the RIP1-Tag2 lesional stages or to a number of normal tissues.

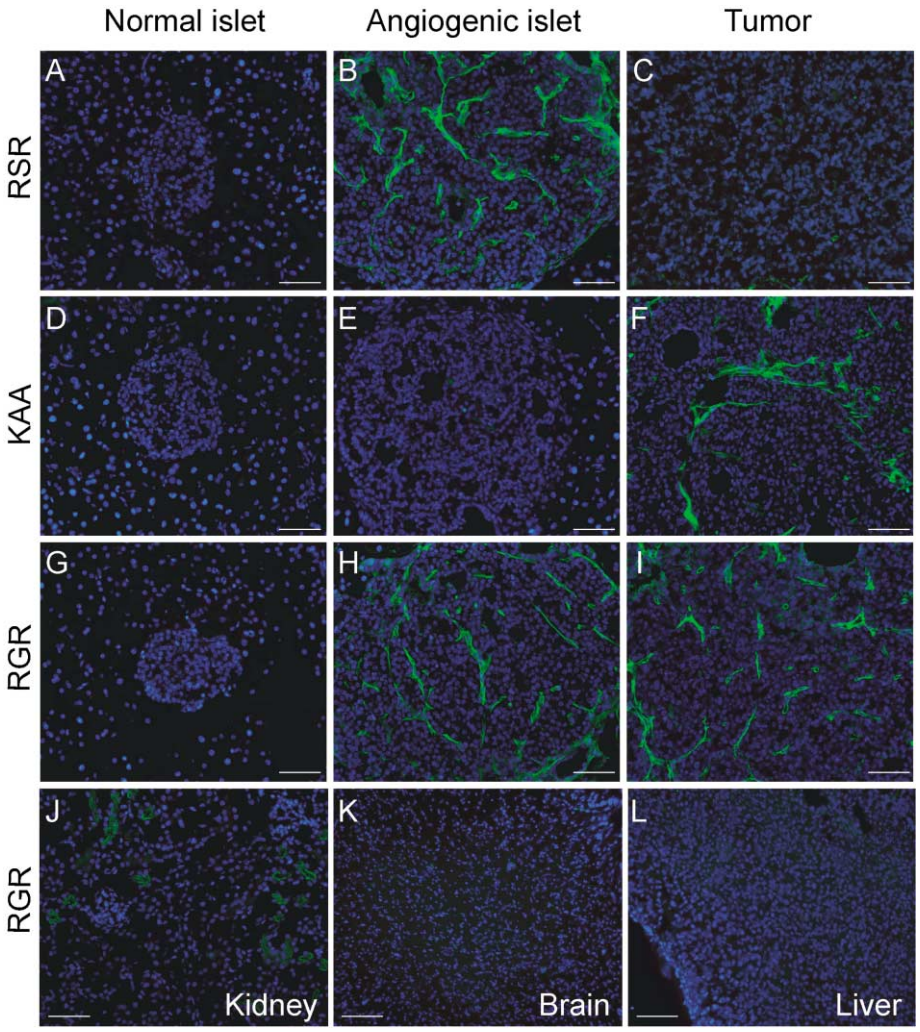


**Figure 2.** Stage-specific homing of fluorescein-conjugated peptides in RIP1-Tag2 model

Visualization of an angiogenic islet-selective peptide (RSR) homing is shown in normal islet (**A**), angiogenic islet (**B**), and tumor (**C**). Homing profiles are also shown for a tumor-selective peptide (KAA) to normal islet (**D**), angiogenic islet (**E**), and tumor (**F**), as well as of a peptide (RGR) that homes to both angiogenic islets and tumors (**G**, normal islet; **H**, angiogenic islet; and **I**, tumor). Control tissues (**J**, kidney; **K**, brain; and **L**, liver) from a RIP1-Tag2 mouse injected with fluorescein-conjugated RGR peptide are also presented. Similar absence of fluorescence in control tissues was observed for all other injected peptides, indicative of a lack of specific homing. The scale bar corresponds to 50 μM.

**Fluorescein-conjugated peptides colocalize with vascular markers**

We reasoned that intravenous administration of the phage libraries would select for phage carrying peptides that bind to endothelial molecules specific for the target vasculature. The expectation of endothelial selectivity is based upon the preferential exposure of phage to luminal cells of the vasculature, as well as the appreciable size of the phage and the short time the phage are allowed to circulate (Pasqualini and Ruoslahti, 1996). In order to test this expectation, tissues were collected following i.v. infusion with the various fluorescein-conjugated peptides, sectioned, and evaluated with endothelial cell markers. The primary analysis involved immunostaining with a mouse pan-endothelial cell antigen (MECA32) antibody that recognizes a dimer of 50–55 kDa protein subunits present on all endothelial cells (Hallman et al., 1995; Leppink et al., 1989) (Figures 3B, 3C, 3H, 3I, 3N, and 3O). Additional analyses (not shown) involved immunostaining to reveal CD31/PECAM or systemic infusion of a fluorescent-labeled lectin that binds to the endothelial lumen. In addition, tissue sections from peptide-infused mice were stained with an antibody recognizing NG2, a marker of the neovascular pericytes (Schlingemann et al., 1990, 1991) (Figures 3E, 3F, 3K, 3L, 3Q, and 3R). Remarkably, all three peptides (RSR, KAA, and RGR) show some colocalization both with endothelial cell and pericyte markers, indicating that each homes to and binds moieties associated with both cell types (Figure 3 and data not shown). Again, there was no colocalization of these peptides with those same markers in the adjacent exocrine pancreas or in normal pancreatic islets; tissue sections stained with MECA32 and NG2 showed some colocalization, consistent with the proximity of endothelial cells and pericytes (Figures 3S–3U).

The apparent homing of peptides representing all three classes of stage specificity to both pericytes and endothelial cells was unexpected. It may be pertinent that the RIP1-Tag2 tumor vasculature is known to be leaky, as evidenced by extensive microhemorrhaging (Parangi et al., 1995) and morphometric analysis (Hashizume et al., 2000; Morikawa et al., 2002; Thurston et al., 1998), such that the circulating phage pool likely had access to the extraluminal vascular microenvironment, where receptors on pericytes and in the extracellular matrix could be accessible. It is known that the vasculature of both angiogenic islets and tumors is leaky (Morikawa et al., 2002). However, reciprocal homing of the peptides that recognize the angiogenic islet but not tumor vessels, and vice versa, excludes the possibility that the recognition of angiogenic islet versus tumor vessels would simply be caused by differences in the leakiness of the

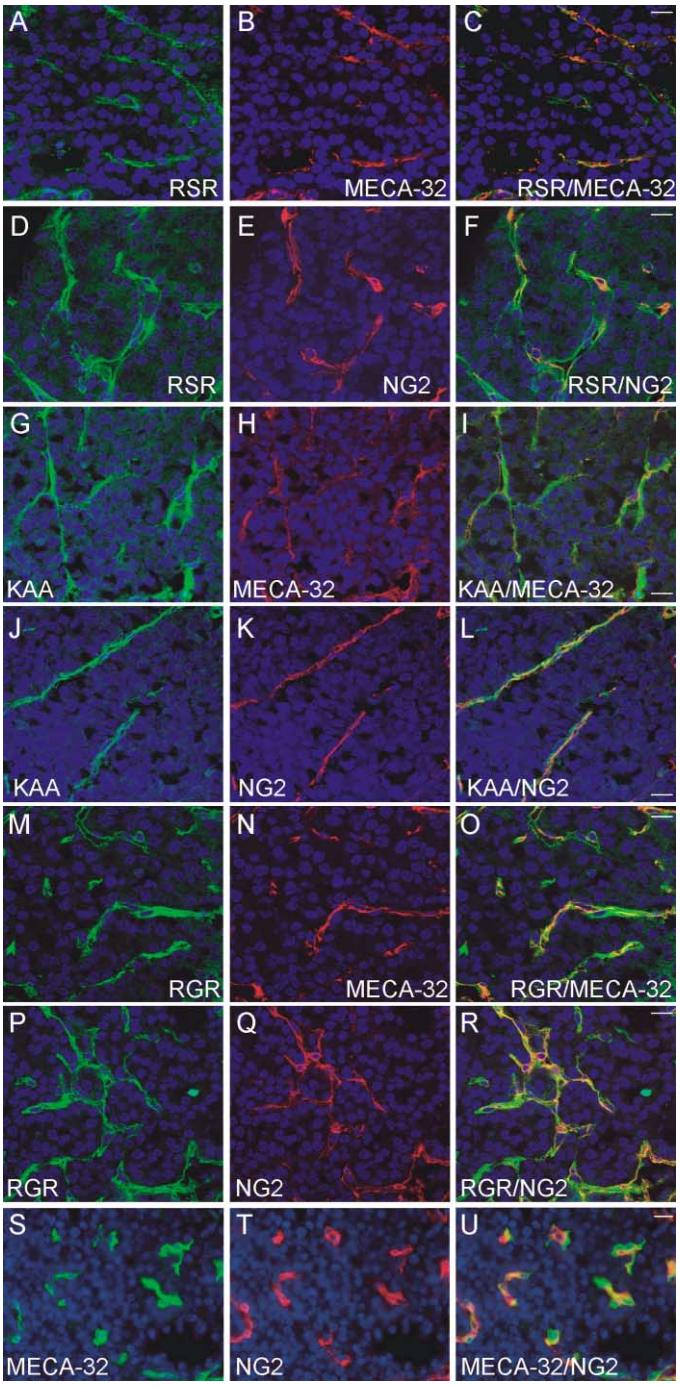


**Figure 3.** Colocalization of fluorescein-conjugated peptides with vascular markers in RIP1-Tag2 islet lesions

RSR peptide localization in an angiogenic islet is shown in (**A**) and (**D**) (green), while co-staining for MECA32 (red) and the merge are shown in (**B**) and (**C**). Co-staining for NG2 (red) is shown in (**E**), with the merge in (**F**). KAA peptide localization in a tumor is shown in (**G**) and (**J**) (green), while co-staining for MECA32 (red) and the merge are shown in (**H**) and (**I**). Co-staining for NG2 (red) is shown in (**K**), with the merge in (**L**). RGR peptide localization in an angiogenic islet is shown in (**M**) and (**P**) (green), while co-staining for MECA32 (red) and the merge are shown in (**N**) and (**O**). Co-staining for NG2 (red) is shown in (**Q**), with the merge in (**R**). Staining for endothelial cells (MECA32) (**S**) and pericytes (NG2) (**T**) in tumor sections demonstrated their close association (**U**). Scale bar: 10 μm.

vessels. The ex vivo pre-selection step we used to enrich for RIP1-Tag2-specific targets may have similarly selected for non-luminal endothelial binding partners, but it should be emphasized that any peptide selected ex vivo must also have been accessible via the circulation during the in vivo selections. Consistent with this logic, phage-displaying peptides that bind to the pericyte marker, NG2, have previously been shown to home to a transplant tumor in vivo (Burg et al., 1999).

### Specificity of in vivo homing to islet tumors in the pancreas

Selection of phage that home to the vasculature of neoplastic lesions in RIP1-Tag2 mice can be envisioned to identify two classes of peptides: those whose cognate receptors are specific to angiogenic islets and/or tumors in the pancreas and those that also home to the angiogenic vasculature in other tumor types. Therefore, we asked whether phage and peptides selected in pancreatic neoplasias would home to two different transplant tumors growing subcutaneously or to de novo skin tumors induced in another transgenic mouse model.

βTC3 transplant tumors arise following subcutaneous inoculation of nude mice with cultured islet tumor-derived (βTC3) cells (Efrat et al., 1988), allowing the study of islet tumors and their vasculature outside of their natural environment in the pancreas. Because the vasculature of a subcutaneously grown βTC3 tumor derives from skin, we also tested another subcutaneous transplant tumor, arising from inoculation of the MDA-MB-435 human breast carcinoma cell line. Finally, K14-HPV16 mice, another well-studied transgenic mouse model of cancer that develop tumors of the squamous epithelial cells of the skin (Arbeit et al., 1994; Coussens et al., 1996), allowed us to compare RIP1-Tag2 islet tumors to a tumor with similar multistage pathogenesis arising in a different tissue. The relative homing efficiencies in the various tumor models of the phage from the RIP1-Tag2 tumor screen fall broadly into two categories: those that selectively home to RIP1-Tag2 tumors (KAA, RGR, VGVA) and those that show a more general homing to other tumors in addition to RIP1-Tag2 (VGVG, KAR) (Figure 4A). The phage homing data were supported by i.v. injection of fluorescein-conjugated peptides corresponding to the phage. Results for the three representative peptides are summarized in Figure 4B, and an example of the tissue fluorescence produced following injection of the KAR peptide in different tumors is shown in Figures 4C–4E.

Homing during non-tumor angiogenesis was examined using angiogenesis in subcutaneously implanted matrigel plugs. All peptides except one showed no homing to the matrigel plugs. The RGR peptide appeared in a punctate manner in some blood vessels. However, the intensity was much lower and the pattern quite different than in RIP-Tag lesions (data not shown). This indicates that this set of peptides are selective for neovascularization during tumorigenesis and are not general markers of neovessel formation.

### Identification of candidate vascular receptors

The set of peptides homing to angiogenic neoplasias in the pancreas were applied to database searches, seeking to identify mouse proteins with sequences homologous to the peptides. Table 1 lists candidate proteins with such homologies that were deemed to be of interest. In theory, these proteins could correspond to putative ligands mimicked by the phage-displayed

A

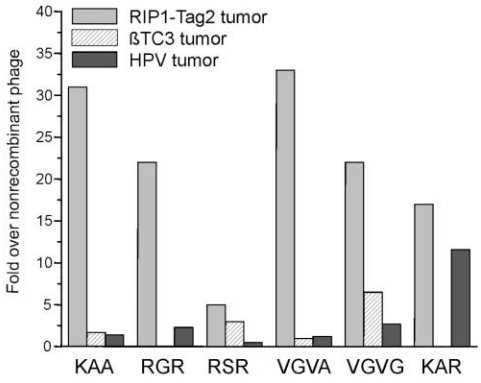


B

| Peptide \ Tumor | RIP1-Tag2 | ßTC3 | HPV | MDA |
|---|---|---|---|---|
| RGR | ++ | - | +/- | - |
| KAA | +++ | +/- | - | +/- |
| RSR | +/- | +/- | - | - |

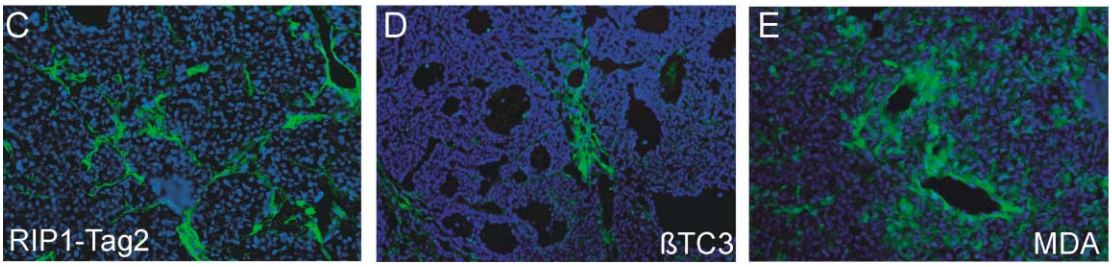


**Figure 4.** Evaluation of the neoplastic specificity of selected homing phage and peptides

**A:** Bar graph showing homing efficiency of individual phage to a pancreatic islet tumor in a RIP1-Tag2 mouse, a βTC3-derived subcutaneous transplant tumor in a nude mouse, and a squamous cell carcinoma in a K14-HPV16 mouse.

**B:** Table summarizing the relative homing of fluorescein-conjugated peptides to different tumor models. +++ indicates strong homing, as revealed by the fluorescent intensity of i.v. injected peptide, ++ indicates moderate homing, + indicates weak homing, - indicates absence of homing. Representative images of fluorescein-conjugated KAR peptide homing to a RIP1-Tag2 pancreatic islet tumor (**C**), a βTC3 subcutaneous tumor (**D**), and an MDA subcutaneous tumor (**E**) are also shown. Magnification 200×.

peptides. Many of the candidate proteins have been previously associated with the vasculature. One protein, collagen XII, was found to share homology with two peptides: KAR (CKGAKAR) and VGVA (FRVGVADV), though in different structural domains. It is interesting to note that collagen XII was also identified by gene expression profiling as a gene that is overexpressed in tumor endothelial cells (St. Croix et al., 2000; and http://mendel.imp.unvie.ac.at/SEQUENCES/TEMS/mainpgs/temtable.html).

It was somewhat surprising that homologies to peptide sequences in two cell surface receptors, fibroblast growth factor receptor 1 (FGFR1) and Tie-1, were revealed by homology searching, as phage-displayed peptides have traditionally been thought to mimic ligands not receptors. However, in the case of FGFR1, the particular peptide sequence (YQLDV) has been reported to be in the ligand binding domain D2 (Plotnikov et al., 1999), suggesting the possibility that the phage displaying this peptide may in fact be binding to FGFR1 ligands, i.e., the fibroblast growth factors (FGFs). It is well known that many of the

**Table 1.** Candidate mouse proteins sharing motifs with homing peptides

| Peptide | Peptide sequence | Extended motif | Mouse protein with the motif | Accession number |
|---|---|---|---|---|
| RGR | CRGRRST | RGRRS | PDGF-B | P31240 |
| | | RGRR | Stromal interaction molecule 2 | Q9P246 |
| RSR | CRSRKG | CRSR-G | Cadherin EGF LAG receptor 1 | O35161 |
| KAA | CKAAKNK | CKA-K | WNT-2 | NPO76142 |
| KAR | CKGAKAR | CKGAKA | Collagen XII | Q60847 |
| | | AKAR | Collagen XII | Q60847 |
| | | GAKAR | Claudin 9 | Q9ZOS7 |
| VGVA | FRVGVADV | F-VGVADV | Collagen XII | Q60847 |
| | | RVGV | Collagen XII | Q60847 |
| EYQ | CEYQLDVE | CEYQL | Semaphorin 4C | Q64151 |
| | | YQLDV | FGFR1 | P16092 |
| | | YQLDV | Tie-1 | Q06806 |

Peptides were analyzed using a BLAST (NCBI) search against the SWISSPROT database, using the option for short nearly exact matches, to identify mouse proteins with homologous sequences.

heparin binding FGFs are sequestered in the extracellular matrix and basement membrane by binding to heparan sulfate proteoglycans (Ornitz and Itoh, 2001), which is consistent with phage homing to these FGF depots in vivo. As the Tie-1 receptor is an orphan receptor tyrosine kinase, ligand binding information is not currently available; however, the peptide sequence homology is in the extracellular domain (Sato et al., 1993).

Another provocative homology was seen for the RGR peptide (CRGRRST), which is contained within the B chain of the pro-form of platelet-derived growth factor (PDGF-B), a known ligand for the transmembrane receptor tyrosine kinase PDGFRβ. The RGR sequence homology (RGRRS) spans the pro-peptide cleavage site of pro-PDGF-B (Johnsson et al., 1984). To investigate the hypothesis that the RGR peptide was homing to PDGFRβ by virtue of this homology, we transfected 293T cells with a fusion gene designed to overexpress PDGFRβ. The binding of RGR phage was 20-fold more efficient to PDGFRβ-transfected cells than nontransfected cells. In contrast, no binding above the background was detected toward cells transfected with vascular endothelial growth factor receptor 2 (VEGFR2) (Figure 5A). Moreover, when we tested the RSR phage, which has a peptide sequence similar to RGR, no specific binding was observed either to PDGFRβ- or VEGFR2-transfected cells (Figure 5A). The association of RGR with PDGFRβ was further substantiated when intravenously injected fluorescein-conjugated RGR peptide was shown to colocalize with PDGFRβ, visualized by subsequent immunostaining of tissue sections from RIP1-Tag2 tumors. Merging of the RGR-FITC image (Figure 5B, panel a) with the antibody staining for PDGFRβ (Figure 5B, panel b) revealed almost complete colocalization (Figure 5B, panels c and d).

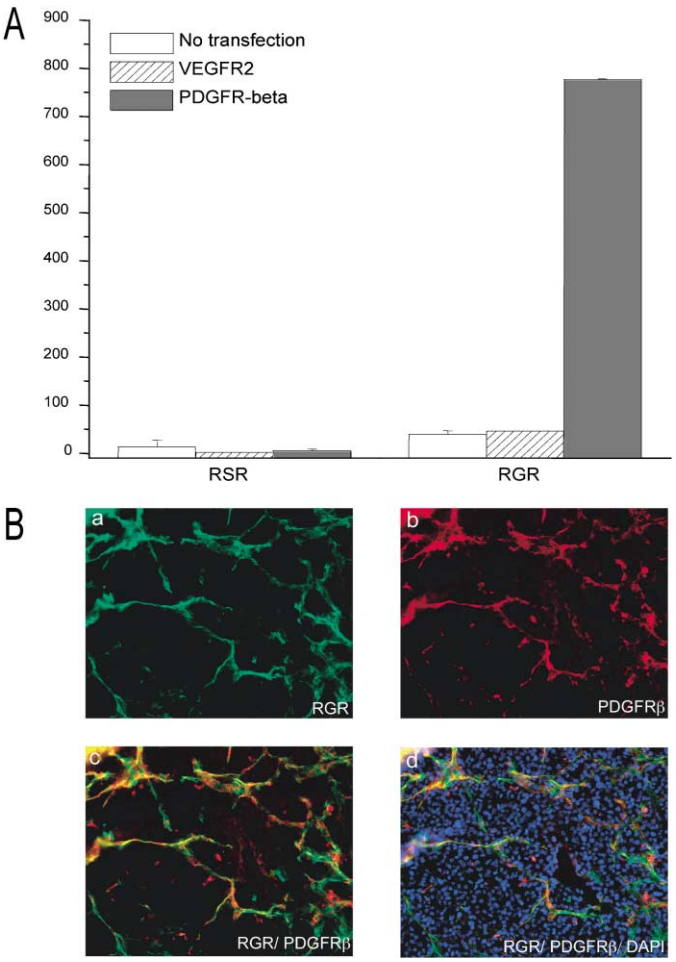


**Figure 5.** PDGFRβ is a candidate receptor for RGR peptide

**A:** Bar graph showing binding of RGR or RSR phage to 293T cells transfected with either the PDGFRβ, the related VEGFR2, or nontransfected cells. Y axis = fold over nonrecombinant phage.

**B:** Colocalization of fluorescein-conjugated RGR peptide (**a**, green) with the PDGFRβ antibody (**b**, red) and merged images (**c** and **d**) in RIP1-Tag2. Magnification 400×.

## Discussion

We set out in this and the companion study (Hoffman et al., 2003) to characterize the vasculature during the discrete stages of organ-specific carcinogenesis, using a profiling technology based on peptide libraries displayed on the surface of bacteriophage. Phage that display a peptide with an appropriate binding specificity home via the circulation to the site of binding affinity. As such, phage profiling can reveal differences in the composition and properties of the vasculature of different organs and pathological lesions. Using as a target the RIP1-Tag2 mouse model of multistage tumorigenesis involving the pancreatic islets of Langerhans, we have identified peptides that discriminate between the vasculature of the premalignant angiogenic islets and the fully developed tumors. Most of the identified homing peptides appear to selectively detect vascular changes induced during tumorigenesis in the endocrine pancreas, but not in other tumors growing in or under the skin. Remarkably, three peptides representing one of the distinctive homing classes (to angiogenic progenitors, to tumors, or to both) each colocalized with markers separately identifying endothelial cells and pericytes in the angiogenic lesions. The sequences of the homing peptides suggest candidate proteins containing homologous sequences that are mimicked by peptide binding to the angiogenic vasculature.

### Insights into organ-specific differences in neoplastic vasculature

The influence of tissue microenvironment in tumor development is increasingly appreciated (Coussens and Werb, 2002; Liotta and Kohn, 2001). As developing neoplasias activate angiogenesis and recruit a neovasculature from the surrounding tissue microvascular bed, the organ microenvironment may influence the morphology and physiology of the tumor neovasculature. Evidence in support of organ-specific differences has come, for example, by comparing permeability in the vessels of transplant tumors as a function both of tumor type and the host tissue site (Hobbs et al., 1998; Roberts et al., 1998).

We asked whether tumors arising in their natural microenvironment are different from those developing in another "foreign" location by comparing endogenously arising RIP1-Tag2 tumors in the pancreas with βTC3 cell-derived tumors grown subcutaneously (the βTC3 cell line was established from a RIP1-Tag2 pancreatic islet tumor; Efrat et al., 1988). The results from both phage and peptide binding (Figure 4 and data not shown) indicate that some phage/peptides home to βTC3 subcutaneous tumors in addition to RIP1-Tag2 endogenous tumors, albeit less efficiently (e.g., VGVG). However, most of the other phage/

peptides do not show any appreciable homing to βTC3 tumors by comparison to RIP1-Tag2 tumors (e.g., KAA and VGVA), supporting the predominant role of the tissue microenvironment in influencing some of the receptors that are displayed on the cell surface.

Similar results were found for the two other tumor types we studied: squamous cell carcinomas of the epidermis arising in K14-HPV16 transgenic mice and subcutaneous xenograft tumors of the human MDA-MB-435 breast cancer cell line. KAR and VGVG were the only phage/peptides that homed appreciably to these models, whereas the other peptides showed a similar lack of homing, as for βTC3 tumors. Thus, the majority of phage-displayed and soluble peptides homed selectively to the tumor vasculature of RIP1-Tag2 tumors arising in their natural environment in the endocrine pancreas, showing little affinity for tumors growing subcutaneously or in the skin itself. By contrast, in the aforementioned study of tumor endothelial genes revealed by expression profiling (St. Croix et al., 2000), a number of the tumor-specific endothelial genes identified as upregulated in a colorectal cancer screen were also found in the tumor endothelium of other cancers (lung, brain, pancreas, and breast primary tumors; and a colorectal metastasis to the liver). Our method has clearly revealed a partially overlapping but distinctive set of markers. These results support the existence of both tumor-specific and tumor-generic vascular markers and may have implications for interpretation of data forthcoming from xenograft tumor models. If vascular markers are not recapitulated in transplant models representing a particular organ-specific cancer, then aspects of its phenotypic behavior and response to therapy (particularly targeted antiangiogenic and antivascular agents) may differ as well. Similar results have been seen in the companion study (Hoffman et al., 2003) comparing de novo epidermal squamous cell carcinomas in the K14-HPV16 mice with transplant tumors in the adjacent subcutaneous microenvironment.

**Homing peptides revealing molecular anatomy of tumor vasculature**

We have begun to investigate candidate binding moieties ("receptors") for the RIP1-Tag2 homing peptides, initially by searching protein databases for proteins that contain the homing peptide sequences and thus might represent the endogenous protein mimicked by the peptide. It is striking that a number of the candidate proteins revealed by the search have been implicated in some aspect of angiogenesis (PDGFs, WNTs, claudins, collagen XII, FGFR1, Tie-1). We chose to evaluate the PDGF-B homology in light of recent evidence implicating PDGF signaling in the angiogenic phenotype in the RIP-Tag2 model: three PDGF ligand genes are expressed in the tumor endothelial cells, while PDGF receptor β is expressed in tumor pericytes (Bergers et al., 2003). Pharmacological inhibition of PDGFR signaling in RIP1-Tag2 mice disrupted pericyte association with the tumor endothelium, inhibited angiogenesis, and reduced the vascularity of the islet tumors (Bergers et al., 2003). The results add to a knowledge base implicating PDGF signaling in pericyte-endothelial cell homeostasis, both in developing vessels (Betsholtz et al., 2001; Leveen et al., 1994; Lindahl et al., 1997; Soriano, 1994) and in tumors (Heldin and Westermark, 1999; Ostman and Heldin, 2001).

The evaluation of RGR in light of its homology to PDGF-B clearly suggests its homing is associated with PDGFR expression and/or signaling. The most compelling evidence comes from overexpressing PDGFRβ in cultured cells. There was a striking increase in the binding of the RGR phage to cells transfected with PDGFRβ, whereas transfection with a structurally related receptor tyrosine kinase, VEGFR2, had no effect on the binding. Moreover, systemically infused RGR colocalizes with virtually all of the PDGFRβ detected by immunostaining in angiogenic islets and tumors. Both lines of evidence support the model that RGR binds to PDGFRβ. There are, however, other data that complicate this simple conclusion. First, RGR colocalizes not only with a pericyte marker, NG2, consistent with PDGFRβ expression in pericytes, but also with an endothelial cell marker, MECA32, indicative of homing to endothelial cells (which do not typically express PDGFRβ—see Bergers et al., 2003). Second, the RGR peptide sequence overlaps the propeptide processing site and is thus only partially represented in mature PDGF-B ligand; moreover, the sequences for PDGF homo- and heterodimerization and for receptor binding are not at the N terminus of the mature ligand (Clements et al., 1991; Heldin and Westermark, 1999; Ostman et al., 1991). Thus it is not clear how RGR might bind either to PDGF ligands or receptors. These data lead us to suggest that RGR mimics a protein-protein interaction site in pro-PDGF-B that mediates its specific homing and mimics bona fide associations of pro-PDGF-B. One possible association for RGR is either with PDGFRβ itself or with a protein induced by its expression, given the enhanced binding seen in the transfected cells overexpressing PDGFRβ as well as the observed colocalization of RGR with PDGFRβ in angiogenic islets and tumors. It is interesting to note that a similar sequence is found in PDGF-D, a related PDGF ligand that also signals through PDGFRβ. The sequence RGRS is located in the secreted PDGF-D at the site of processing from the inactive to active form of PDGF-D (Bergsten et al., 2001; LaRochelle et al., 2001).

The additional colocalization of RGR with the endothelial cell marker MECA32 suggests that an RGR binding moiety is also expressed by endothelial cells or shared between pericytes and endothelial cells. While there is no obvious coimmunostaining of either endothelial cell marker (CD31, MECA32) with any of several pericyte markers (desmin, SMA, NG2) in the angiogenic islets or tumors (J.J. and G.B., unpublished observations), a small subset of FAC-sorted cells within RIP1-Tag2 tumors are positive for both CD31 and NG2 (G.B., unpublished observations). In addition, both cell types contribute to the vascular basement membrane and the extracellular matrix that separates and envelops them, and these structures could contain RGR binding motifs produced by one or both cell type and localized amongst them. Indeed, purified PDGF-B has been shown to bind various ECM and BM proteins, including collagens I–IV (Somasundaram and Schuppan, 1996), laminin-1, nidogen, and perlecan (Gohring et al., 1998). Another attractive candidate for RGR binding is the predicted prohormone processing enzyme that binds and cleaves pro-PDGF-B within the RGR homology. Interestingly, while the RGR phage and peptide homed effectively to angiogenic progenitor islets and solid tumors in RIP1-Tag2 mice, neither homed to angiogenic dysplasias or tumors in the HPV16 transgenic mice nor to the MDA-MB-435 subcutaneous tumors. These results suggest that PDGF signaling and the resultant vessel stabilization by pericytes may differ among tumors or that there are differences in pericyte activation and/or maturation (Morikawa et al., 2002). Alternatively, the blood

vessels in the squamous cell carcinomas, being less hemorrhagic, may limit the accessibility of the blood-borne phage and labeled peptides to the perivascular cells (see below).

Other homologies between homing peptides and endogenous proteins listed in Table 1 may also be significant. The fact that many of these proteins have been implicated in angiogenesis, or related biological processes, supports this prediction. For example, two of the peptides, KAR and VGVA, show homology to collagen XII, which is associated with blood vessels in the developing embryo (Bohme et al., 1995; Oh et al., 1993). Colocalization of both peptides with vascular markers (data not shown) is consistent with the predicted localization of collagen XII.

**Lessons from profiling different tumor types**

It is of interest to compare and contrast the results reported here to that of the companion study (Hoffman et al., 2003), which similarly used phage display libraries to profile the angiogenic dysplasias and squamous cell carcinomas that arise in the skin of K14-HPV16 transgenic mice. That study produced a series of homing peptides that were selective for angiogenic progenitors or solid tumors. And again, both tumor type-selective and tumor-generic phage were identified; their analysis focused on skin tumor-specific phage that did not home to the angiogenic vasculature in the stages of pancreatic islet carcinogenesis in RIP1-Tag2 mice. The skin-tumor homing peptides had different sequences from those identified herein, and their candidate cellular homologs (and prospective binding moieties) were distinctive. In sum, each study identified both tumor type-specific and stage-specific vascular homing peptides, further supporting the proposition that organ microenvironment imparts distinctive constraints on neoplastic development that affects the characteristics of the neovasculature induced to sustain tumor development and progression.

It is intriguing that the two organ sites of neoplastic development (skin and pancreas) preferentially selected phage with different cellular specificity. The HPV phage all homed exclusively to endothelial cells, whereas each of the RIP1-Tag2 phage representing the three homing classes (angiogenic progenitor, tumor, or both) chosen for analysis homed both to pericytes and to endothelial cells. This suggests significant differences in the vascular morphology and/or functionality in the skin and pancreas. One difference may be in vascular permeability. The islet tumors are blood red from hemorrhaging and the angiogenic vasculature is permeable to a variety of macromolecules (Hashizume et al., 2000; Thurston et al., 1998). By contrast, the skin tumors are white, indicative of less hemorrhagic vessels or higher interstitial pressure. Thus the phage population circulating through the vascular system in RIP1-Tag2 mice may have had ready access to the perivascular microenvironment, whereas the "tighter" vessels in the skin lesions may limit such accessibility. Future studies on the expression of the "receptors" identified by these distinctive classes of homing peptides should clarify whether their binding moieties are differentially expressed and/or differentially accessible via the vasculature in these distinctive tumor types and their angiogenic progenitor lesions, providing further insight into the dynamics and tissue-specific qualities of the angiogenic phenotype.

The selective accumulation of fluorescein-conjugated peptides in the RIP-Tag lesions indicates that a monovalent peptide-receptor interaction is robust enough to carry a payload to the target. As such, these peptides could be used as biomarkers or for imaging, particularly of pre-neoplastic lesions, which are notoriously difficult to detect. The peptides homing to angiogenic islets, for example, could be used both as markers of the angiogenic switch and to monitor therapeutic response to antiangiogenic agents, in much the same way as parameters such as microvessel density are currently employed. Future experiments will test the efficacy of targeting of imaging agents and active drugs to multiple stages of tumorigenesis.

In conclusion, we have used phage display to profile the vasculature during the distinctive stages of multistep tumorigenesis in a prototypical mouse model of cancer. We have identified three different classes of stage-specific peptides suggestive of distinctive characteristics of the neovasculature in premalignant and malignant lesions. We expect that the selectivity in peptide homing will help us understand the stage-specific differences in efficacy observed for angiogenesis inhibitor therapy in the RIP1-Tag2 model (Bergers et al., 1999). In addition, it may be possible to selectively target antitumor therapies to individual or multiple cell types during RIP-Tag tumorigenesis using these homing peptides conjugated to, for example, proapoptotic sequences, as previously reported (Ellerby et al., 1999). It will be of further interest to ask whether these homing peptides can similarly characterize the neovasculature of stages in human pancreatic islet carcinogenesis, as well as in other organ-specific cancers in mouse models and humans.

## Experimental procedures

### Generation of mice and tissue isolation

The generation of RIP1-Tag2 mice (Hanahan, 1985) and K14-HPV16 mice (Arbeit et al., 1994; Coussens et al., 1996) has been reported. Angiogenic islets were isolated from 8- and 12-week-old RIP1-Tag2 mice by collagenase digestion of the excised pancreas and selected based on their red, hemorrhagic appearance (Parangi et al., 1995). Tumors were microdissected from the excised pancreas of 12-week-old RIP1-Tag2 mice and the surrounding exocrine tissue was carefully removed. The synchronicity of tumorigenesis in the RIP1-Tag2 model allowed us to simultaneously isolate pools of angiogenic islets and tumors from the same mouse at 12 weeks of age, thus affording us the opportunity to directly compare homing of individual phage to different stages in an individual mouse/pancreas. Tumors were dissected from the ear or chest of K14-HPV16 mice. For the βTC3 allograft models, $10^6$ βTC3 tumor cells (Efrat et al., 1988) were inoculated under the skin of the rear flank of *nu/nu* mice in a BALB/c background and allowed to grow until approximately 5 mm in size, and then used for experimental analysis. MDA-MB-435 xenograft models were generated by inoculating $10^6$ tumor cells subcutaneously in the chest of *nu/nu* BALB/c mice. Tumors were used for the homing/binding experiments at 8–12 weeks after injection of the tumor cells. Matrigel plug angiogenesis was induced as previously described (Fulgham et al., 1999; Ngo et al., 2000; Yi et al., 2003). Briefly, 100 μl of Matrigel containing 80 ng/ml bFGF was injected subcutaneously in the abdominal area of BALB/c/*nu/nu* mice, and at day 8, the mice were injected with fluorescein-conjugated peptides as detailed below.

### Phage libraries and library screening

The screening process involved two ex vivo selection rounds followed by 2–3 in vivo selection rounds. For the ex vivo selections, cell suspensions were prepared from the different RIP1-Tag2 lesions in 12-week-old RIP1-Tag2 mice and incubated overnight at 4°C with $10^9$ plaque forming units (p.f.u.) of a T7 phage (Novagen) displayed $CX_7C$ peptide library. The cells were washed to remove unbound phage and the bound phage rescued and amplified in *E. coli*. This procedure enriches for phage that bind to tumor, endothelial, and other stromal cells present in the suspension. The ex vivo pre-selected phage pool was injected intravenously into 12-week-old RIP1-Tag2 mice through the tail vein, allowed to circulate for 7 min, and heart-perfused with PBS to remove unbound intravascular phage. As the vascula-

ture is preferentially available for the phage to bind in this selection, there is an enrichment of phage that bind to the endothelium of the target tissue. The RIP1-Tag2 lesions and control tissues (brain, kidney, spleen, lung, "white" pancreas [i.e., not containing any hemorrhagic lesions], and liver) were excised to allow for comparison of homing efficiencies. Cell suspensions were prepared by mechanical disruption of the tissues, washed to remove unbound phage, and the bound phage rescued and amplified by adding *E. coli*. The phage pool was reinjected into mice at a similar disease stage, and the cycle repeated. In each experiment, nonrecombinant control phage was used as a control for relative selectivity. Sets of 96 phage clones were randomly collected from each homing phage population. The peptide-encoding DNA inserts were amplified by PCR, and the PCR products sequenced. Phage representing the most frequently appearing peptide motifs were individually tested for their ability to selectively home to the lesions on which they were selected, relative to other stages in the tumorigenesis pathway and to control organs. Fluorescein-conjugated peptides corresponding to these phage insert sequences were synthesized using an automated peptide synthesizer with standard solid-phase fluorenylmethoxycarbonyl (Fmoc) chemistry. One hundred micrograms of each individual fluorescein-conjugated peptide was injected intravenously into the tail vein of RIP1-Tag2 mice at 8 or 12 weeks of age and into normal BL/6 mice. The peptide was allowed to circulate for 7 min, followed by heart perfusion first with PBS and then with Zn-buffered formalin. The RIP1-Tag2 pancreas and control organs (brain, kidney, liver, lung, and spleen) were removed, fixed for 1 hr in formalin, washed with 1× PBS, placed in 30% sucrose for several hours, washed with 1× PBS, and embedded in OCT (Tissue-Tek). Each peptide was injected into at least three individual RIP1-Tag2 or normal mice at each of the different stages.

**Histology and immunohistochemistry**

To examine the localization of injected fluorescein-conjugated peptides, frozen sections (10 μm thick) were cut on a cryostat, mounted in Vectashield Mounting Medium with DAPI (Vector Laboratories), and visualized under an inverted fluorescent microscope or a confocal microscope (Zeiss LSM 510 META). For immunohistochemistry, frozen slides were preincubated with blocking buffer (1× PNB from NEN Biosciences) for 1 hr, washed several times in 1× PBS, and incubated with the primary antibody of interest overnight at 4°C. The cell-specific antibodies used were rat monoclonal anti-mouse CD31 (1:200; BD Pharmingen), rat monoclonal anti-mouse MECA32 (1:200; BD Pharmingen), rabbit polyclonal anti-mouse NG2 (1:200; Chemicon), and rat monoclonal anti-mouse PDGFRβ (CD140b) (1:200; eBioscience). The corresponding secondary antibodies; Cy-3 donkey anti-rabbit IgG and Rhodamine Red donkey anti-rat IgG (Jackson ImmunoResearch), were used at a 1:200 dilution and incubated for 1 hr at room temperature. The following species-matched immunoglobulins were used as negative controls: rabbit IgG (Vector Laboratories) and rat IgG (Jackson ImmunoResearch) at a 1:200 dilution. The slides were washed several times in 1× PBS and mounted in Vectashield Mounting Medium with DAPI (Vector Laboratories). Hematoxylin and eosin (H&E) staining was performed for histological grading of adjacent sections by standard methods, and lesions were graded as previously described (Lopez and Hanahan, 2002).

**Transfection and phage binding assay**

293T cells were transfected with plasmids encoding PDGFRβ or VEGFR2 (Borges et al., 2000) using Fugene transfection reagent (Roche Diagnostics). Briefly, 10 μg of plasmid was mixed with 700 μl of DMEM without serum and 30 μl of Fugene and incubated for 15 min at room temperature before adding the mixture to the cells. Forty-eight hours posttransfection, the cells were detached from the culture plates using EDTA and washed 1× with PBS. RSR, RGR, and the control nonrecombinant phage (about $1 \times 10^9$ pfu) were incubated with the transfected cells for 2 hr at 4°C, followed by five washes with 1% BSA in PBS to remove the unbound phage. The bound phage were rescued by adding bacteria, and the binding efficiencies were determined by plaque assay.

**Acknowledgments**

We thank Cherry Concengco for excellent technical assistance and Fernando Ferrer for peptide synthesis. We thank Dr. Kristian Pietras for reading the manuscript and for helpful suggestions. This study was supported by a grant from the National Cancer Institute CA82713 (to E.R. and D.H.) and by grants from the Department of Defense DAMD 17-02-1-0315 (E.R.) and the N.C.I. (D.H.). J.A.J. received support from the Leukemia and Lymphoma Society. P.L. received support from the Academy of Finland and the Finnish Cultural Foundation.

Received: June 5, 2003
Revised: September 10, 2003
Published: November 24, 2003

**References**

Arap, W., Pasqualini, R., and Ruoslahti, E. (1998). Cancer treatment by targeted drug delivery to tumor vasculature in a mouse model. Science *279*, 377–380.

Arbeit, J., Munger, K., Howley, P.M., and Hanahan, D. (1994). Progressive squamous epithelial neoplasia in K14-human papillomavirus type 16 transgenic mice. J. Virol. *68*, 4358–4368.

Bergers, G., Hanahan, D., and Coussens, L.M. (1998). Angiogenesis and apoptosis are cellular parameters of neoplastic progression in transgenic mouse models of tumorigenesis. Int. J. Dev. Biol. *42*, 995–1002.

Bergers, G., Javaherian, K., Lo, K.M., Folkman, J., and Hanahan, D. (1999). Effects of angiogenesis inhibitors on multistage carcinogenesis in mice. Science *284*, 808–812.

Bergers, G., Song, S., Meyer-Morse, N., Bergsland, E., and Hanahan, D. (2003). Benefits of targeting both pericytes and endothelial cells in the tumor vasculature with kinase inhibitors. J. Clin. Invest. *111*, 1287–1295.

Bergsten, E., Uutela, M., Li, X., Pietras, K., Ostman, A., Heldin, C.-H., Alitalo, K., and Eriksson, U. (2001). PDGF-D is a specific protease-activated ligand for the PDGF β-receptor. Nat. Cell Biol. *3*, 512–516.

Betsholtz, C., Karlsson, L., and Lindahl, P. (2001). Developmental roles of platelet-derived growth factors. Bioessays *23*, 494–507.

Bohme, K., Li, Y., Oh, P.S., and Olsen, B.R. (1995). Primary structure of the long and short splice variants of mouse collagen XII and their tissue-specific expression during embryonic development. Dev. Dyn. *204*, 432–445.

Borges, E., Jan, Y., and Ruoslahti, E. (2000). Platelet-derived growth factor receptor beta and vascular endothelial growth factor receptor 2 bind to the beta 3 integrin through its extracellular domain. J. Biol. Chem. *275*, 39867–39873.

Burg, M.A., Pasqualini, R., Arap, W., Ruoslahti, E., and Stallcup, W.B. (1999). NG2 proteoglycan-binding peptides target tumor neovasculature. Cancer Res. *59*, 2869–2874.

Carmeliet, P., and Jain, R. (2000). Angiogenesis in cancer and other diseases. Nature *407*, 249–257.

Clements, J.M., Bawden, L.J., Bloxidge, R.E., Catlin, G., Cook, A.L., Craig, S., Drummond, A.H., Edwards, R.M., Fallon, A., Green, D.R., et al. (1991). Two PDGF-B chain residues, arginine *27* and isoleucine *30*, mediate receptor binding and activation. EMBO J. *10*, 4113–4120.

Coussens, L.M., and Werb, Z. (2002). Inflammation and cancer. Nature *420*, 860–867.

Coussens, L.M., Hanahan, D., and Arbeit, J.M. (1996). Genetic predisposition and parameters of malignant progression in K14–HPV16 transgenic mice. Am. J. Pathol. *149*, 1899–1917.

Efrat, S., Linde, S., Kofod, H., Spector, D., Delannoy, M., Grant, S., Hanahan, D., and Baekkeskov, S. (1988). Beta-cell lines derived from transgenic mice expressing a hybrid insulin gene-oncogene. Proc. Natl. Acad. Sci. USA *85*, 9037–9041.

Ellerby, H.M., Arap, W., Ellerby, L.M., Kain, R., Andrusiak, R., Rio, G.D., Krajewski, S., Lombardo, C.R., Rao, R., Ruoslahti, E., et al. (1999). Anti-cancer activity of targeted pro-apoptotic peptides. Nat. Med. *5*, 1032–1038.

Folkman, J., Watson, K., Ingber, D., and Hanahan, D. (1989). Induction of

angiogenesis during the transition from hyperplasia to neoplasia. Nature *339*, 58–61.

Fulgham, D.L., Widhalm, S.R., Martin, S., and Coffin, J.D. (1999). FGF-2 dependent angiogenesis is a latent phenotype in basic fibroblast growth factor transgenic mice. Endothelium *6*, 185–195.

Gohring, W., Sasaki, T., Heldin, C.H., and Timpl, R. (1998). Mapping of the binding of platelet-derived growth factor to distinct domains of the basement membrane proteins BM-40 and perlecan and distinction from the BM-40 collagen-binding epitope. Eur. J. Biochem. *255*, 60–66.

Hallman, R.D., Mayer, D.N., Berg, E.L., Broermann, R., and Butcher, E.C. (1995). Novel mouse endothelial cell surface marker is suppressed during differentiation of the blood brain barrier. Dev. Dyn. *202*, 325–332.

Hanahan, D. (1985). Heritable information of pancreatic beta-cell tumors in transgenic mice expressing recombinant insulin/simian virus 40 oncogenes. Nature *315*, 115–122.

Hanahan, D., and Folkman, J. (1996). Patterns and emerging mechanisms of the angiogenic switch during tumorigenesis. Cell *86*, 353–364.

Hashizume, H., Baluk, P., Morikawa, S., McLean, J.W., Thurston, G., Roberge, S., Jain, R.K., and McDonald, D.M. (2000). Openings between defective endothelial cells explain tumor vessel leakiness. Am. J. Pathol. *156*, 1363–1380.

Heldin, C.H., and Westermark, B. (1999). Mechanism of action and in vivo role of platelet-derived growth factor. Physiol. Rev. *79*, 1283–1316.

Hobbs, S.K., Monsky, W.L., Yuan, F., Roberts, W.G., Griffith, L., Torchilin, V.P., and Jain, R.K. (1998). Regulation of transport pathways in tumor vessels: Role of tumor type and microenvironment. Proc. Natl. Acad. Sci. USA *95*, 4607–4612.

Hoffman, J.A., Giraudo, E., Singh, M., Zhang, L., Inoue, M., Porkka, K., Hanahan, D., and Ruoslahti, E. (2003). Cancer Cell *4*, this issue, 383–391.

Johnsson, A., Heldin, C.H., Wasteson, A., Westermark, B., Deuel, T.F., Huang, J.S., Seeburg, P.H., Gray, A., Ullrich, A., Scrace, G., et al. (1984). The c-*sis* gene encodes a precursor of the B chain of platelet-derived growth factor. EMBO J. *3*, 921–928.

Laakkonen, P., Porkka, K., Hoffman, J.A., and Ruoslahti, E. (2002). A tumor-homing peptide with a targeting specificity related to lymphatic vessels. Nat. Med. *8*, 751–755.

LaRochelle, W.J., Jeffers, M., McDonald, W.F., Chillakuru, R.A., Giese, N.A., Lokker, N.A., Sullivan, C., Boldog, F.L., Yang, M., Vernet, C., et al. (2001). PDGF-D, a new protease-activated growth factor. Nat. Cell Biol. *3*, 517–521.

Leppink, D.M., Bishop, D.K., Sedmak, D.D., Henry, M.L., Ferguson, R.M., Streeter, P.R., Butcher, E.C., and Orosz, C.G. (1989). Inducible expression of an endothelial cell antigen on murine myocardial vasculature in association with interstitial cellular infiltration. Transplantation *48*, 874–877.

Leveen, P., Pekny, M., Gebre-Medhin, S., Swolin, B., Larsson, E., and Betsholtz, C. (1994). Mice deficient for PDGF-B show renal, cardiovascular and hematological abnormalities. Genes Dev. *8*, 1875–1887.

Lindahl, P., Johansson, B.R., Leveen, P., and Betsholtz, C. (1997). Pericyte loss and microaneurysm formation in PDGF-B deficient mice. Science *277*, 242–245.

Liotta, L.A., and Kohn, E.C. (2001). The microenvironment of the tumour-host interface. Nature *411*, 375–379.

Lopez, T., and Hanahan, D. (2002). Elevated levels of IGF-1 receptor convey invasive and metastatic capability in a mouse model of pancreatic islet tumorigenesis. Cancer Cell *1*, 339–353.

Morikawa, S., Baluk, P., Kaidoh, T., Haskell, A., Jain, R.K., and McDonald, D.M. (2002). Abnormalities in pericytes on blood vessels and endothelial sprouts in tumors. Am. J. Pathol. *160*, 985–1000.

Ngo, C.V., Gee, M., Akhtar, N., Yu, D., Volpert, O., Auerbach, R., and Thomas-Tikhonenko, A. (2000). An in vivo function for the transforming Myc protein: elicitation of the angiogenic phenotype. Cell Growth Differ. *11*, 201–210.

Oh, S.P., Griffith, C.M., Hay, E.D., and Olsen, B.R. (1993). Tissue-specific expression of type XII collagen during mouse embryonic development. Dev. Dyn. *196*, 37–46.

Ornitz, D.M., and Itoh, N. (2001). Fibroblast growth factors. Genome Biol. *2*, 3005.1–3005.12.

Ostman, A., and Heldin, C.H. (2001). Involvement of platelet-derived growth factor in disease: development of specific antagonists. Adv. Cancer Res. *80*, 1–38.

Ostman, A., Andersson, M., Hellman, U., and Heldin, C.H. (1991). Identification of three amino acids in the platelet-derived growth factor (PDGF) B-chain that are important for binding to the PDGF-β receptor. J. Biol. Chem. *266*, 10073–10077.

Parangi, S., Dietrich, W., Christofori, G., Lander, E.S., and Hanahan, D. (1995). Tumor suppressor loci on mouse chromosomes 9 and 16 are lost at distinct stages of tumorigenesis in a transgenic model of islet cell carcinoma. Cancer Res. *55*, 6071–6076.

Pasqualini, R., and Ruoslahti, E. (1996). Organ targeting *in vivo* using phage display peptide libraries. Nature *380*, 364–366.

Pasqualini, R., Koivunen, E., Kain, R., Lahdenranta, J., Sakamoto, M., Stryhn, A., Ashmun, R.A., Shapiro, L.H., Arap, W., and Ruoslahti, E. (2000). Aminopeptidase N is a receptor for tumor-homing peptides and a target for inhibiting angiogenesis. Cancer Res. *60*, 722–727.

Plotnikov, A.N., Schlessinger, J., Hubbard, S.R., and Mohammadi, M. (1999). Structural basis for FGF receptor dimerization and activation. Cell *98*, 641–650.

Porkka, K., Laakkonen, P., Hoffman, J.A., Bernasconi, M., and Ruoslahti, E. (2002). A fragment of the HMGN2 protein homes to the nuclei of tumor cells and tumor endothelial cells *in vivo*. Proc. Natl. Acad. Sci. USA *99*, 7444–7449.

Rajotte, D., Arap, W., Hagedorn, M., Koivunen, E., Pasqualini, R., and Ruoslahti, E. (1998). Molecular heterogeneity of the vascular endothelium revealed by *in vivo* phage display. J. Clin. Invest. *102*, 430–437.

Roberts, W.G., Delaat, J., Nagane, M., Huang, S., Cavenee, W.K., and Palade, G.E. (1998). Host microvasculature influence on tumor vascular morphology and endothelial gene expression. Am. J. Pathol. *153*, 1239–1248.

Ruoslahti, E. (2002). Specialization of tumour vasculature. Nat. Rev. Cancer *2*, 83–90.

Sato, T.N., Qin, Y., Kozak, C.A., and Audus, K.L. (1993). Tie-1 and Tie-2 define another class of putative receptor tyrosine kinase genes expressed in early embryonic vascular system. Proc. Natl. Acad. Sci. USA *90*, 9355–9358.

Schlingemann, R.O., Rietveld, F.J., de Waal, R.M., Ferrone, S., and Ruiter, D.J. (1990). Expression of the high molecular weight melanoma-associated antigen by pericytes during angiogenesis in tumors and in healing wounds. Am. J. Pathol. *136*, 1393–1405.

Schlingemann, R.O., Rietveld, F.J., Kwaspen, F., van de Kerkhof, P.C., de Waal, R.M., and Ruiter, D.J. (1991). Differential expression of markers for endothelial cells, pericytes, and basal lamina in the microvasculature of tumors and granulation tissues. Am. J. Pathol. *138*, 1335–1347.

Somasundaram, R., and Schuppan, D. (1996). Type I, II, III, IV, V, and VI collagens serve as extracellular ligands for the isoforms of platelet-derived growth factor (AA, BB, and AB). J. Biol. Chem. *271*, 26884–26891.

Soriano, P. (1994). Abnormal kidney development and hematological disorders in PDGFβ-receptor mutant mice. Genes Dev. *8*, 1888–1896.

St. Croix, B., Rago, C., Velculescu, V., Traverso, G., Romans, K.E., Montgomery, E., Lal, A., Riggins, G.J., Lengauer, C., Vogelstein, B., and Kinzler, K.W. (2000). Genes expressed in human tumor endothelium. Science *289*, 1197–1202.

Thurston, G., McLean, J.W., Rizen, M., Baluk, P., Haskell, A., Murphy, T.J., Hanahan, D., and McDonald, D.M. (1998). Cationic liposomes target angiogenic endothelial cells in tumors and chronic inflammation in mice. J. Clin. Invest. *101*, 1401–1413.

Yi, M., Sakai, T., Fassler, R., and Ruoslahti, E. (2003). Antiangiogenic proteins require plasma fibronectin or vitronectin for in vivo activity. Proc. Natl. Acad. Sci. USA, in press.